APPLICATION AND COMPARISON OF THE CRS STACK BASED MINIMUM-APERTURE KIRCHHOFF MIGRATION IN TIME AND DEPTH DOMAIN

M. Kienast

email: *Mareike.Kienast@gpi.uka.de*
keywords: *seismics, imaging, CRS, migration, AVO*

ABSTRACT

CRS-based limited-aperture Kirchhoff migration has successfully been adopted in the time as well as the depth domain. Here, both approaches have been applied to a complex real data set to analyse the stability of the methods. In both cases, the migrated image could be improved in areas with stable and reliable attributes. However, the overall image suffers from strong fluctuations in the attributes due to the low S/N ratio of the input data. With respect to the dynamic aspects of migration, the time domain approach yields superior results as it is less sensitive to errors in the migration velocity model. Both methods significantly reduce the computational time.

INTRODUCTION

The stacking parameters of the Common-Reflection-Surface (CRS) stack, the so-called kinematic wavefield attributes, provide important information that have a wide range of applications, here utilised for limited-aperture migration. The aim of the migration with minimum aperture is to reduce migration artefacts and to provide an improved input for subsequent amplitude-versus-offset (AVO) analysis. Jäger (2005) presented the limited-aperture migration in depth domain for the pre- and poststack case. Spinner and Mann (2006) presented the CRS-based limited-aperture in time migration where the sensitivity to model errors is reduced and the operator is smooth and analytic. As the aperture size strongly influences the quality of the migration images and amplitudes, the aim in limited-aperture depth as well as time migration was to restrict the migration aperture size to the size of the projected Fresnel zone.

In this paper, I present the fist application of the time migration with minimum aperture to real data. The kinematic as well as dynamic aspects are considered in the time and the depth domain, and compared to conventional results.

TIME MIGRATION

To gain the kinematic wavefield attributes the highly automated CRS stack method was applied to the real data set. The resulting stacked section is displayed in Figure 1.

The necessary information to determine the velocity model for time migration can be extracted from the coherence, stack, and attribute sections. At 2870 data points with high coherence, attributes were automatically picked and utilised for the construction of the time migration velocity model. Reliable picks could only be determined from CMP nos. 1 to 1225. Beyond this location the velocity model was constantly extrapolated in lateral direction. For a detailed description of time migration velocity model building I refer to Spinner and Mann (2006).

With the attribute-based time migration velocity model, true-amplitude Kirchhoff poststack time migration was performed twice: on the one hand in a conventional way with a user-defined aperture, on the other hand with the limited aperture given by the projected Fresnel zone.

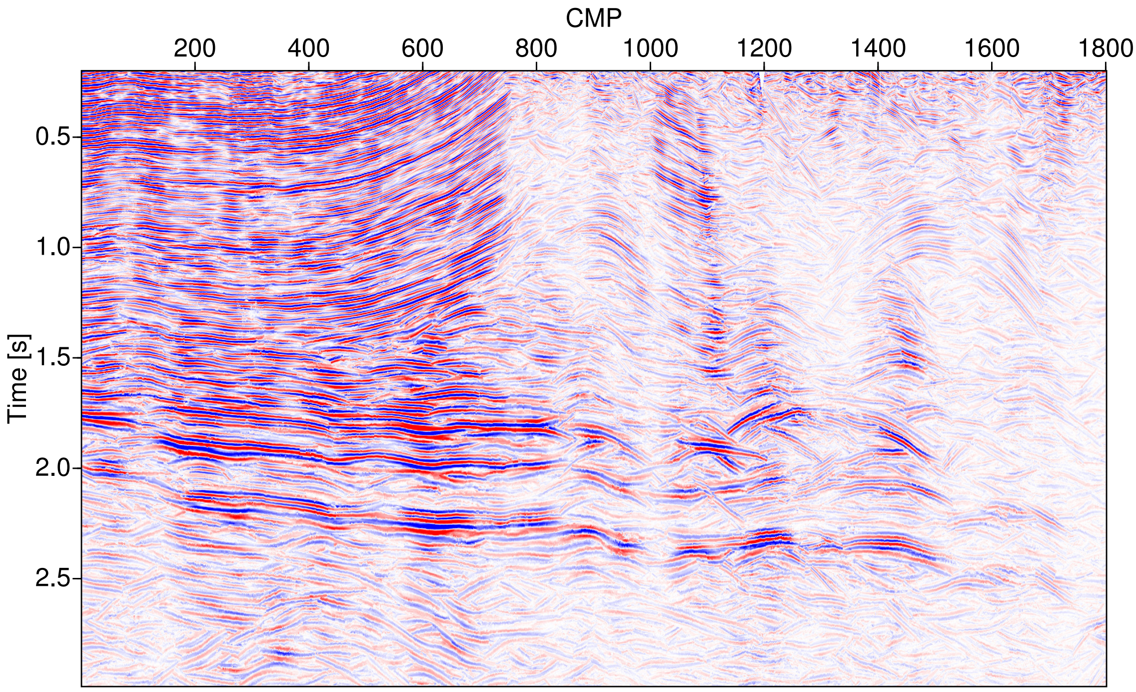

Figure 1: Initial CRS stack section.

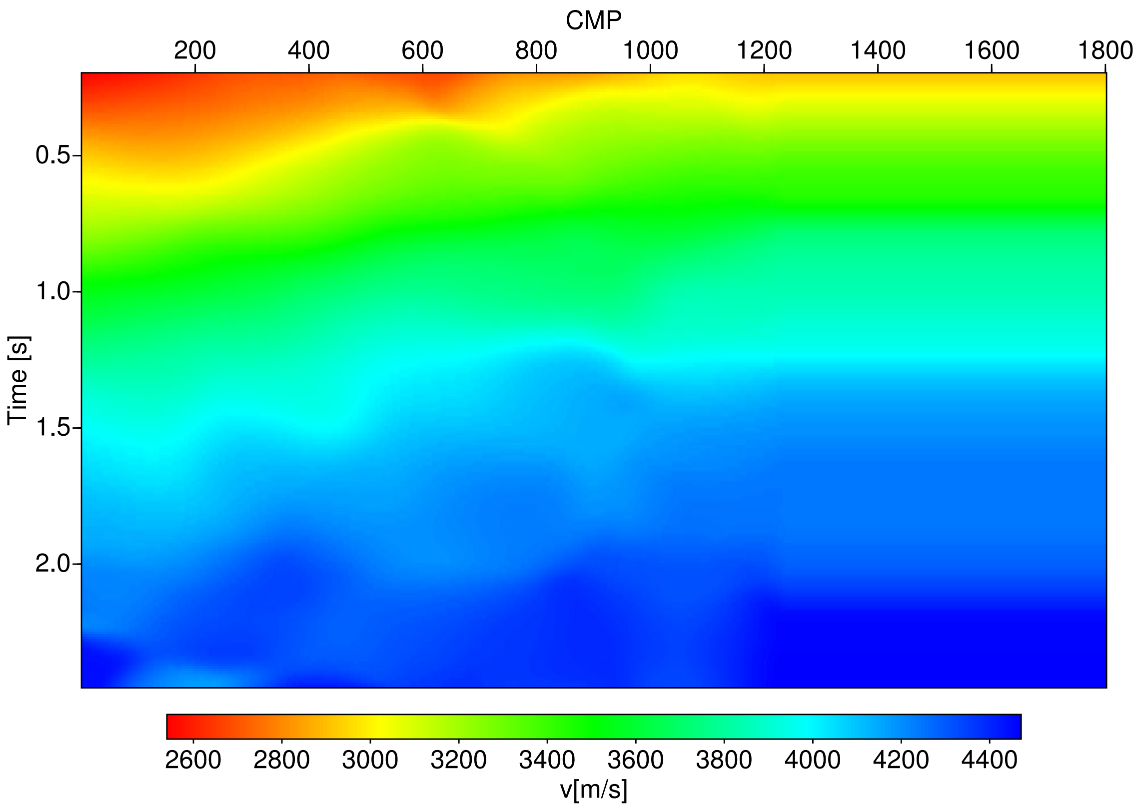

Figure 2: Smoothed time migration velocity model determined from the CRS wavefield attributes

The poststack time migration was processed using the CRS stack section shown in Figure 1 and the determined velocity model (Figure 2). The migration target zone consists of a grid with 25 m spatial and 4 ms temporal intervals. The high temporal resolution was chosen to allow a clear separation of closely adjacent reflection events. For the data at hand, the conventional user-given aperture had to be chosen such that the steeply dipping reflector elements located between CMP nos. 500 and 750 and between 1000 and 1100 could be properly imaged. For both approaches a taper was considered in order to suppress artifacts due to border effects.

For all locations where a stationary point has been detected, Figure 3a) shows the projected Fresnel zone. As expected, its size increases with increasing traveltime and increasing curvature of the reflection events. I observe conspicuously large projected Fresnel zones at various locations. To analyse this effect, I consider the Fresnel zone and the CRS attributes in the unmigrated domain (not displayed). According to the relation between the Fresnel zone size and the CRS attributes, this indicates (fragments of) diffraction events with $R_{\mathrm{N}} \approx R_{\mathrm{NIP}}$. As at such locations there are no evident anomalies in the NIP wave radius which might indicate failures of the search algorithm, this interpretation appears consistent. For these data, conflicting dip handling has not been applied due to the poor signal-to-noise ratio. As a consequence, only one event can be characterised at each ZO location, namely the event associated with the highest coherence. As the steep flanks of (weak) diffraction events interfere with neighbouring reflection events, they often appear as fragments, only. Nevertheless, the local attributes clearly reveal their nature.

In Figure 3b) the horizontal distance between operator apex and stationary point is depicted. It is clearly visible that for flat events the distance tends to zero while on steep events the values of the distance between operator apex and stationary point reach up to 800 m. This demonstrates why a large conventional user-defined aperture is required to capture such events.

Figure 4b) depicts the result of the limited-aperture migration, only performed at locations where stationary points have been detected. Figure 4a) shows that stationary points have been found on all strong events. To obtain a fully covered image without gaps, the user-defined aperture was utilised at all other locations. This result is shown in Figure 5b). For comparison, Figure 5a) displays the result of the conventional poststack time migration.

In the upper part of the two migrated images only minor differences can be seen, even for the events with significant dip. The good performance of the conventional approach in this area can be explained as follows: for the events with small dips, a comparatively small user-given aperture can be used without loss of events. The steeper events show a slightly concave structure that leads to a slight decrease in the Fresnel zone size. Therefore, the projected Fresnel zone is still well covered by the user-given aperture although it is displaced with respect to the operator apex.

A closer investigation of the target reflection events reveals different effects in the limited-aperture migration result: on the one hand, an improved continuity of the target reflection events, for instance at the target reflection event between CMP nos. 200 to 400 at 2.15 s, but on the other hand unphysical fluctuations due to unreasonably strong variations of the attributes occurring around CMP no. 900 at 2.3 s. The imaging problem at this area is also complicated by conflicting dip situations which have, as already mentioned, not been considered for these data. The fluctuations occurring due to varying attributes are usually prevented by a previous event-consistent smoothing of the attributes. However, due to the poor signal-to-noise ratio and low coherence of the data set a reliable smoothing was not possible in this case.

The advantages of limited-aperture time migration in comparison to conventional time migration can be separated into kinematic and dynamic improvements. The kinematic effects are not very distinctive and can be seen in several areas in the migrated image. However, the limited-aperture time migration shows its main advantages with respect to dynamic aspects, as will be shown later on in the context of prestack time migration. As a further advantage, the decreased computing time is resumed in the summary.

The prestack migration is applied just in the same way as poststack migration, with the differences that for prestack migration the whole prestack data set serves as input and that the migration operator is also calculated for finite offset. To perform it in a limited-aperture manner, an additional extrapolation of the stationary point along the approximate CRP trajectory is required.

In Figure 6 several common-image gathers are displayed, extracted at a regular CMP interval from the full conventional prestack migration result. The maximum offset in the data is 3 km. An offset-dependent moveout can be clearly observed for the right hand part of the model where, due to the lack of reliable picks, a constant extrapolation has been used. Of course, no kinematic consistency can be expected under

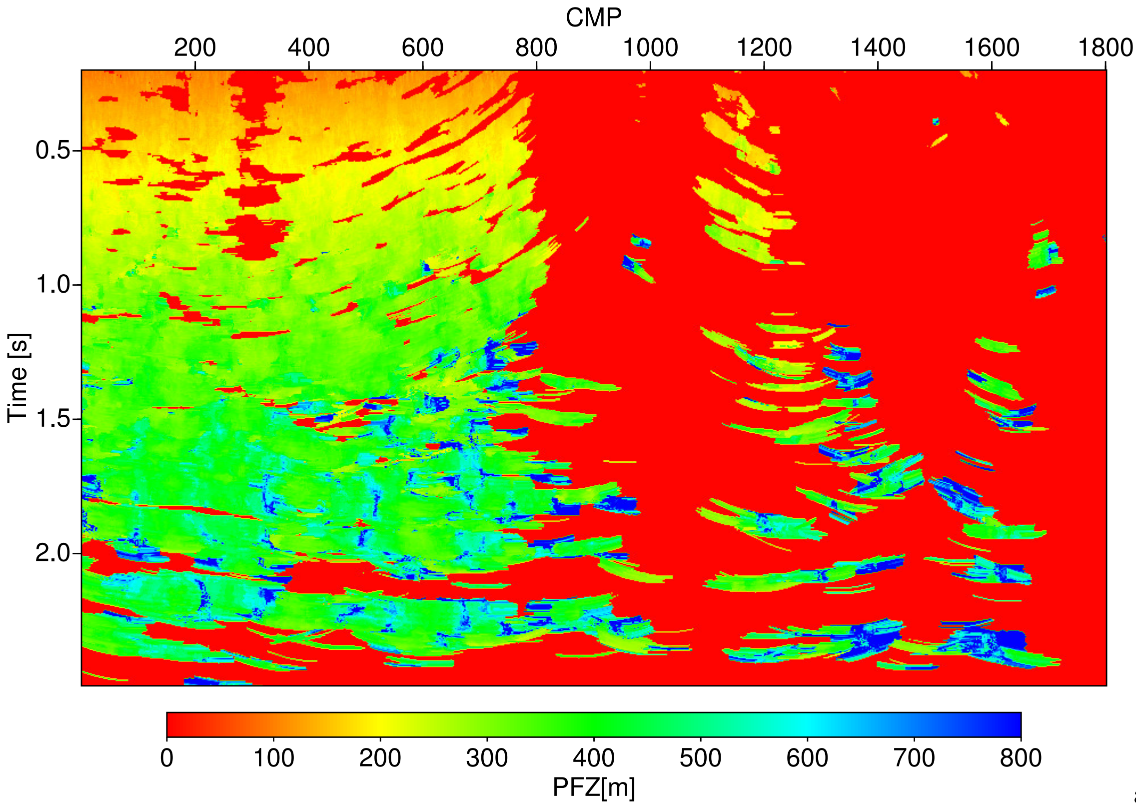

a)

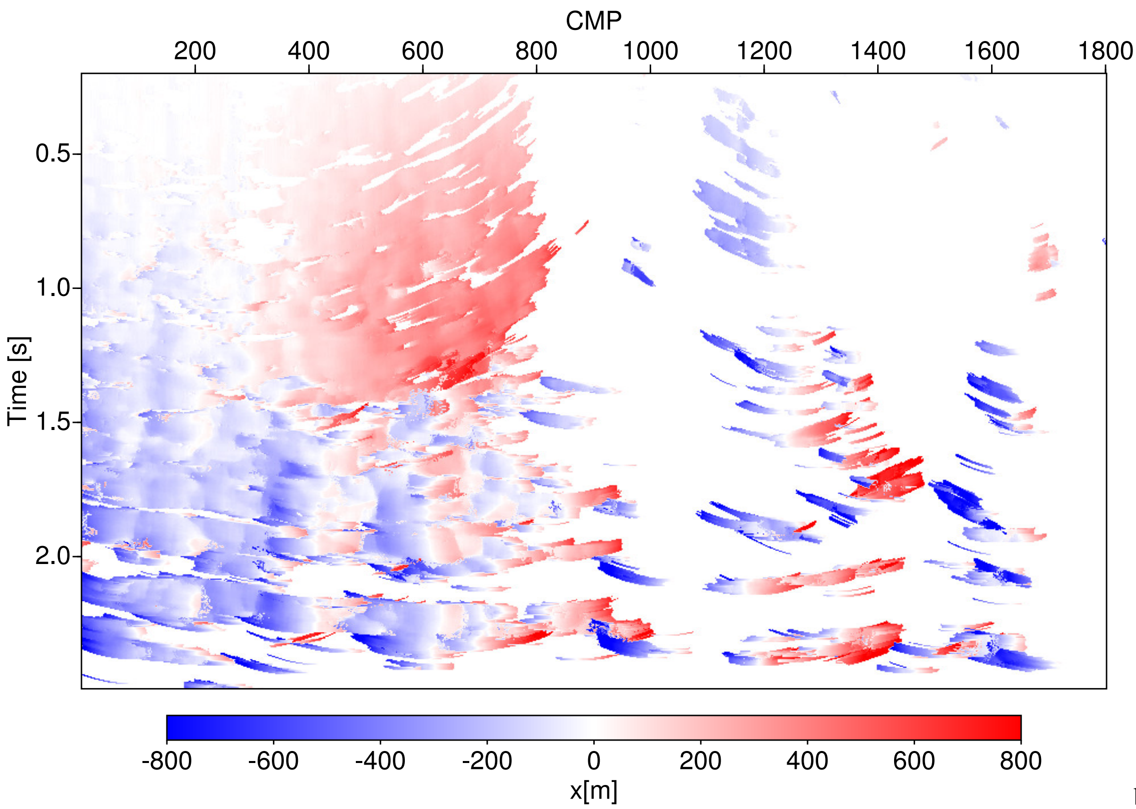

b)

Figure 3: Size of the projected first ZO Fresnel zone estimated from the CRS attributes. Only locations with identified stationary points have been considered a). Horizontal distance between operator apex and stationary point estimated from the CRS attributes b).

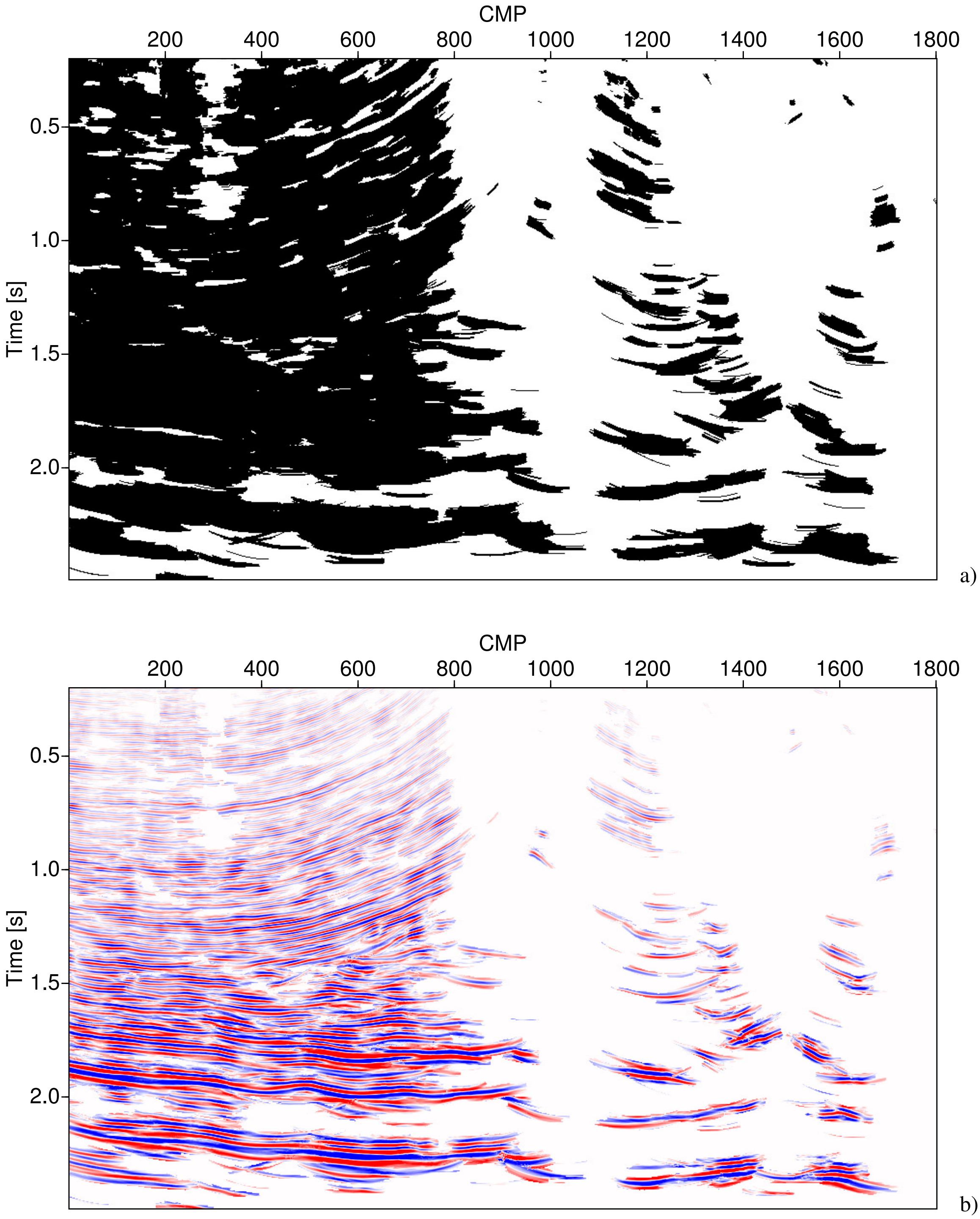

Figure 4: Locations in the migration target zone for which a stationary point has been found (black) a). Only for these locations the limited-aperture poststack migration is performed b).

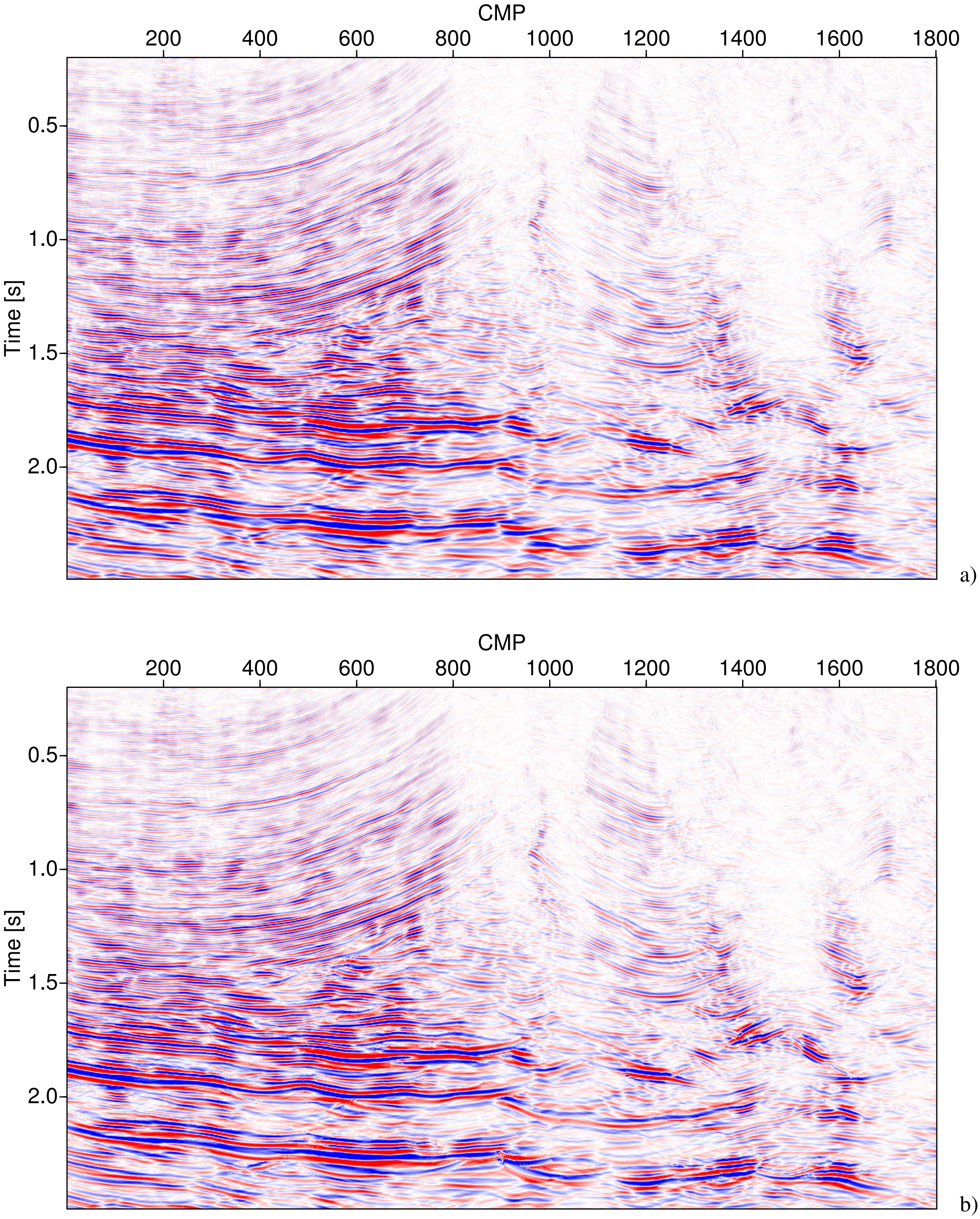

Figure 5: Result of the Kirchhoff poststack time migration with a) conventional user-defined aperture and b) with minimum aperture. The minimum-aperture migration was performed at all locations where a stationary point has been found. At all other locations the user-given aperture is used.

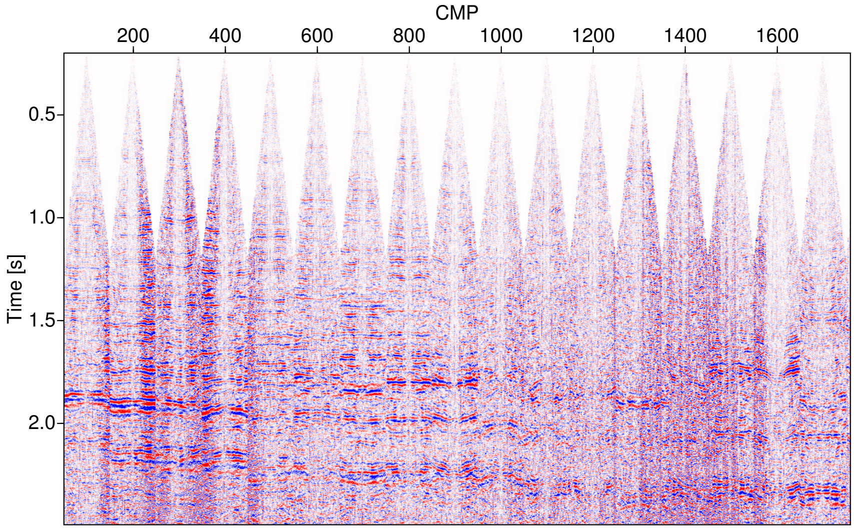

Figure 6: Several common-image gathers extracted from the conventional time migration prestack data. The maximum offset is 3 km. Many events are horizontal while others show a moveout. Thus, the velocity model used for time migration can still be improved.

such conditions where the model is not directly constrained by the picked data.

Figure 7a) shows the conventional migration result after muting and stacking over all offsets, whereas in Figure 7b) the corresponding result of the prestack migration with minimum aperture is depicted. As in the poststack case, the user-defined aperture was used at all locations where no stationary point was found. The differences between the two prestack results are comparable to those of the poststack results. Again, the continuity of the target reflection events has improved in certain areas like on the second target reflector around CMP no. 370. However, also unphysically varying attributes have been detected in areas, e. g., around 2.3 s and CMP no. 1600.

The difficulty of limited-aperture migration is to find an appropriate coherence threshold which controls the search for the attributes and stationary points. In an ideal but unrealistic case only reliable and stable attributes are detected while at the same time stationary points are detected on every reflection event. In this data set, the poor signal-to-noise ratio and low coherence demands a trade-off between coverage with stationary points and their reliability. In order to get the best limited-aperture migration result under consideration of the above described facts, I calculated several prestack results with different coherence thresholds. The impact upon the migrated images is displayed in Figure 8. As expected, more stationary points are detected when the coherency threshold value is smaller. The examples show that coherency thresholds below 0.1 produce truncated reflection events at CMP nos. 1450 to 1550 at 1.7 to 1.85 s, associated to unreliable attributes. The fluctuations due to strongly varying attributes increases also with coherency thresholds of 0.05 and 0.02. Using a value above 0.1 leads to the loss of stationary points referring to obvious reflection events. The migration result depicted in Figure 8e), processed with a coherency threshold of 0.1 gave the best measure between coverage and reliability.

After the discussion of the kinematic effects in limited-aperture time migration, now the dynamic aspects are examined. The effect on the amplitudes was analysed by extracting AVO curves, allowing a further characterisation of the target reflectors. Therefore, amplitudes were extracted from a strong reflector in the common-image gather at CMP 560 in both, conventional and limited-aperture prestack migration results. The resulting AVO curves are depicted in Figure 9. The fluctuations of the amplitudes in the AVO curves are due to noise in the input data. A reduction of the fluctuations can be observed in the limited-aperture AVO plot, as just the relevant part of the data was summed up in this approach. Hence, AVO analysis benefits from migration with limited aperture.

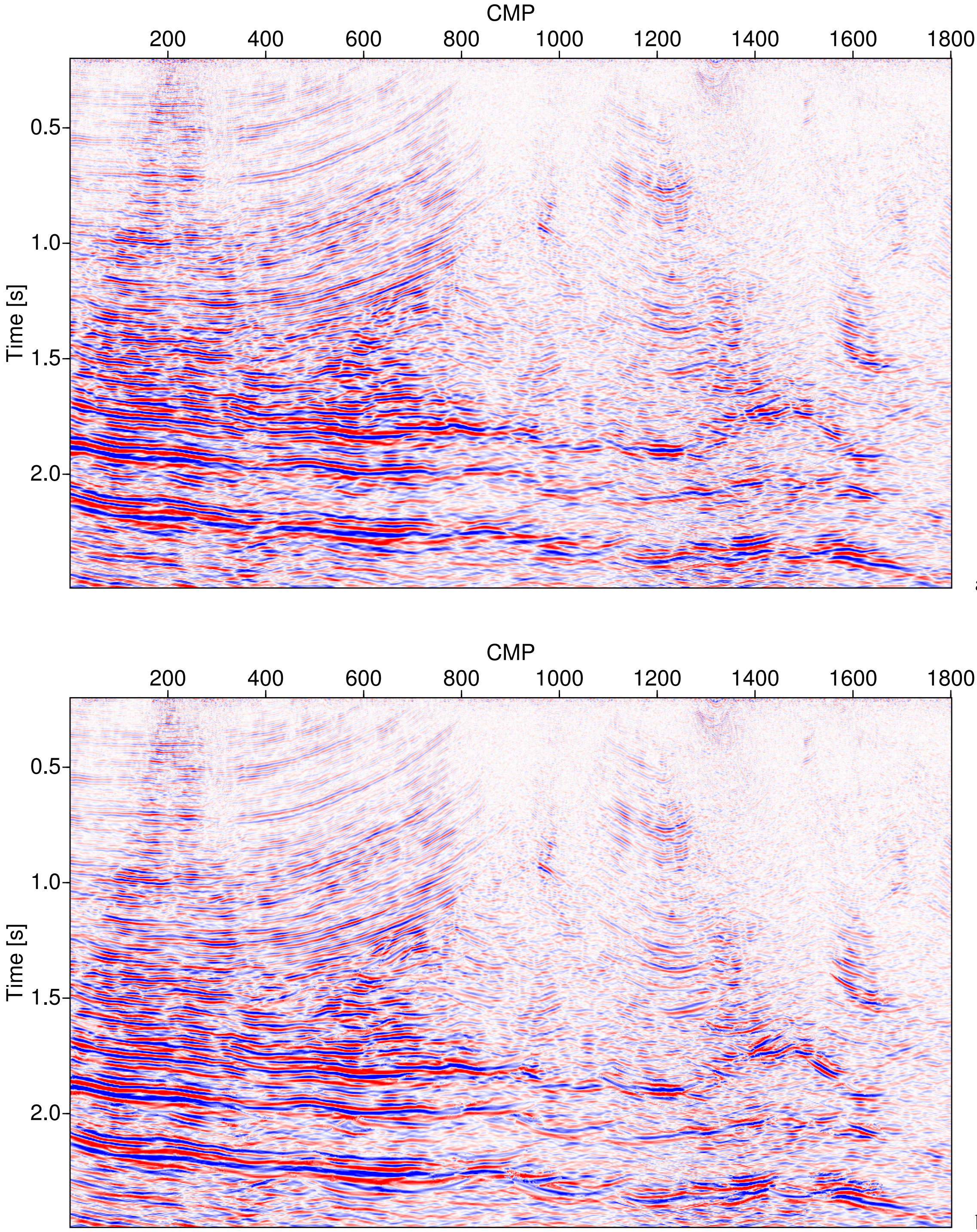

a)

b)

Figure 7: Result of the Kirchhoff prestack time migration with a) conventional user-defined aperture and b) with minimum aperture. The minimum-aperture migration was performed at all locations where a stationary point has been found. At all other locations the user-given aperture is used.

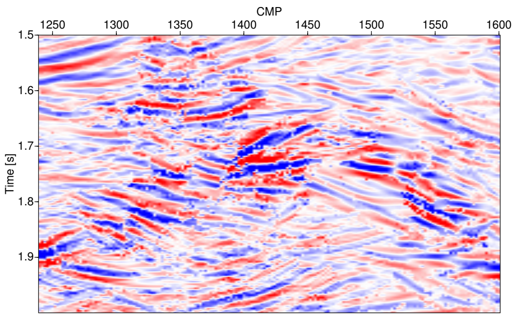

(a) Detail of the limited-aperture time migration result with a coherence threshold of 0.02.

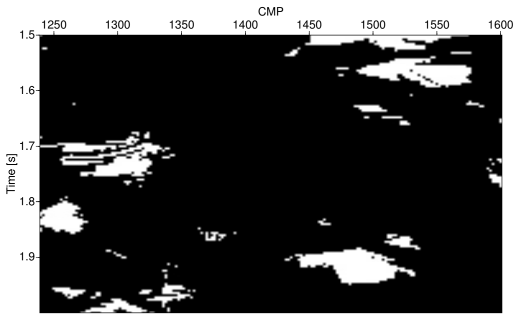

(b) Detail of the limited-aperture time migration mask with a coherence threshold of 0.02. The black points indicate the locations in the migration target zone for which a stationary point has been found.

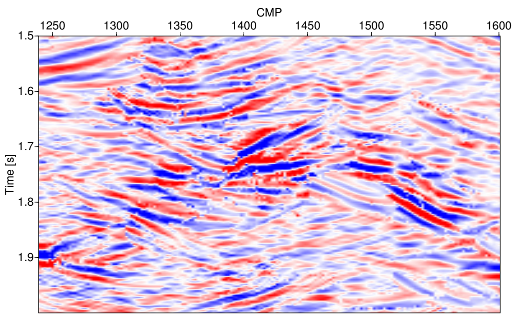

(c) Same detail, but processed with a coherency threshold of 0.05.

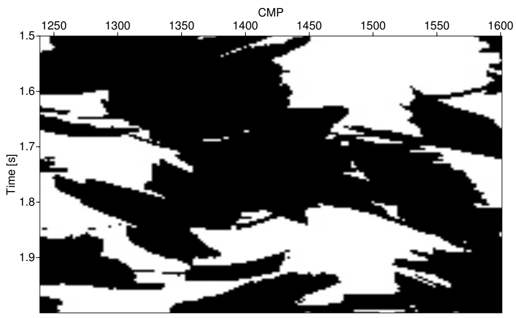

(d) Points in the migration target zone, processed with a coherency threshold of 0.05, for which a stationary point has been found.

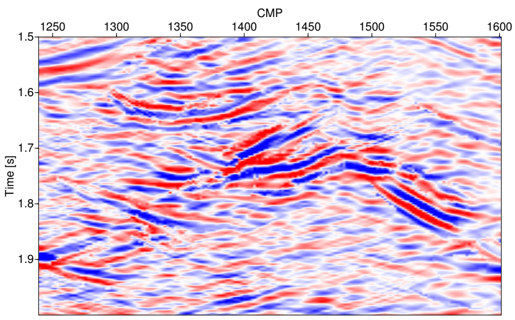

(e) Detail of figure 7b) with a coherence threshold of 0.1.

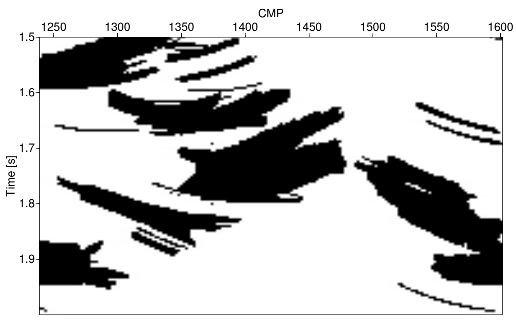

(f) The corresponding stationary points detected of the limited-aperture time migration with a coherency threshold of 0.1.

Figure 8: Comparison of the limited-aperture results with different coherence thresholds.

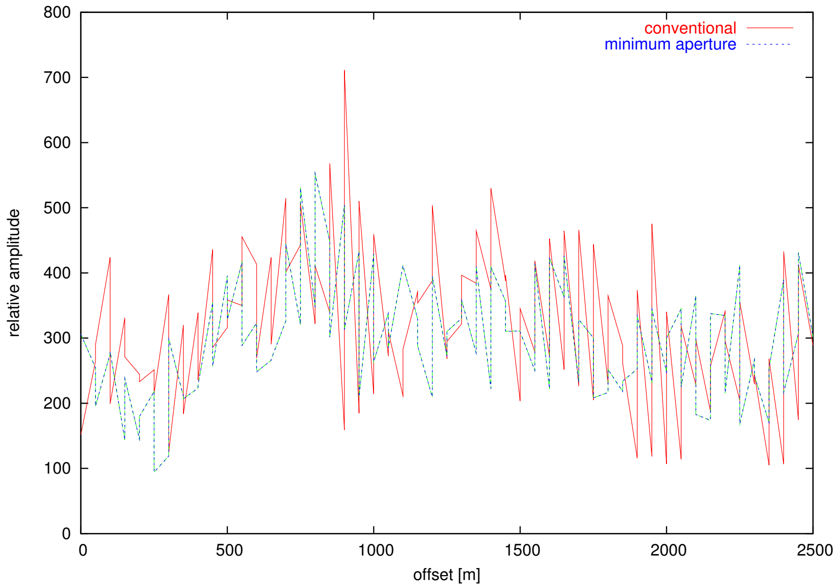

Figure 9: AVO of a strong reflector event at 1.8 s extracted in the common-image gather for CMP no. 560 after true-amplitude prestack time migration with minimum aperture (dashed line) and conventional aperture (solid line). Due to noise in the input data set the amplitudes fluctuate. With minimum aperture the fluctuations are smaller.

DEPTH MIGRATION

The required smooth macro-velocity model for depth migration was determined from the coherence, stack, and attribute sections.

The automatically picked attributes, described for time migration velocity building, were also utilised for the construction of depth migration velocity model. The velocity model, parameterised by two dimensional B-Spline functions, consists of 450 knots, with 45 knots in x-direction with an interval of 500 m and in z-direction 10 knots with an interval of 300 m. The determined velocity model after 9 iterations is shown in Figure 10. A detailed description of depth migration velocity building can be found in Duveneck (2004).

Again the results of the prestack and poststack depth migration with either conventional migration or limited-aperture migration will be shown.

The true-amplitude Kirchhoff poststack depth migration was performed using the CRS stack section shown in Figure 1 and the determined velocity model (Figure 10). The migration target zone was defined by a grid with 25 m lateral and 4 m depth intervals. Again, the minimum aperture was given by the Fresnel zone while the aperture for conventional migration was user-defined and chosen such that all steeply dipping reflector elements could be properly imaged. For both approaches a taper was applied to suppress artefacts caused by border effects.

Figure 11a) shows all points in the migration target zone for which a stationary point was found. The image resulting after limited-aperture migration is displayed in Figure 11b). Again, to obtain a fully covered migration image, the user-given aperture was applied at all other locations where no stationary point was found. The complete poststack depth migrated result is depicted in Figure 12b). For comparison the result of the conventional poststack depth migration is displayed in Figure 12a).

The distinct differences between the two poststack depth migration results can be seen on the target reflectors. The continuity of the reflection events at areas like in between CMP nos. 200 to 400 at 4.4 km have improved in the migration image calculated with minimum aperture. At the location around CMP no. 900 at all three target reflectors a conflicting dip situation is observed. As discussed in time migration only the event associated with the highest coherency is displayed in such cases. Comparing the upper part of the migration images, the conventional result is very similar to the limited-aperture result. Again, this can be

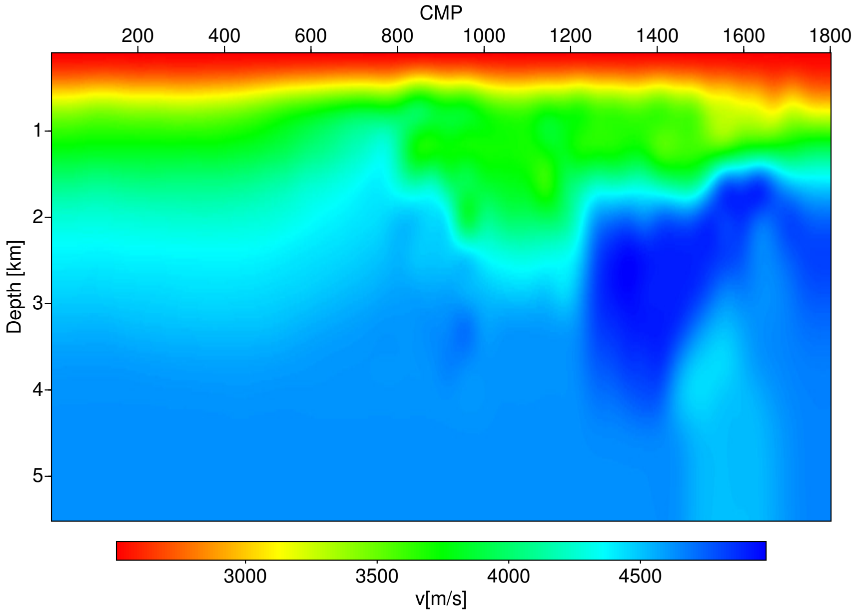

Figure 10: Smoothed depth migration macro-velocity model determined from the CRS-attribute-based tomographic inversion.

explained by the fact that the Fresnel zone is well covered by the user-given aperture in this area.

In order to evaluate the kinematic consistence of the determined velocity model with the data, some common-image gathers were extracted at a regular CMP interval from the conventional prestack migration result. Figure 13 shows the common-image gathers with a maximum offset of 3 km. As described before, the lack of reliable picks, especially at CMP nos. 850 to 1800, explains the offset-dependent moveout.

The conventional Kirchhoff prestack depth migration result shown in Figure 14a) was generated after muting and stacking the migrated prestack data in offset direction. For comparison, Figure 14b) depicts the (fully covered) prestack depth migrated result for minimum aperture.

In general, prestack depth migration shows an increased sensitivity to errors in the migration velocity model. This also holds for the minimum-aperture approach which explains the less distinctive improvements in the prestack migration result.

Testing the impact of minimum aperture in depth migration upon the amplitudes, AVO curves were extracted along the same strong reflector as in the time migration. The fluctuations in the resulting AVO curves of Figure 15 are due to the noise in the input data. The effect from the incorrect depth migration velocity model on the amplitudes obscures the effect of the different apertures considered for migration. Therefore, no clear differences can be seen between the two AVO curves.

COMPUTING TIME

In general, the computation time for time migration is reduced compared to depth migration, as the migration operator is analytic. Both cases additionally benefit from limiting the aperture.

- Time migration:
  - Prestack time migration: the limited-aperture prestack time migration result was obtained in half of the computation time of the prestack migration with conventional aperture. For a sound comparison of the run times all limited-aperture migrations were produced as full covered images without gaps, using the user-defined aperture at all locations where no stationary point was found. This significant decrease in the computation time has its reason in the smaller aperture, reducing the number of required summations.
  - Poststack time migration: in the poststack case the limited-aperture migration is faster, too.

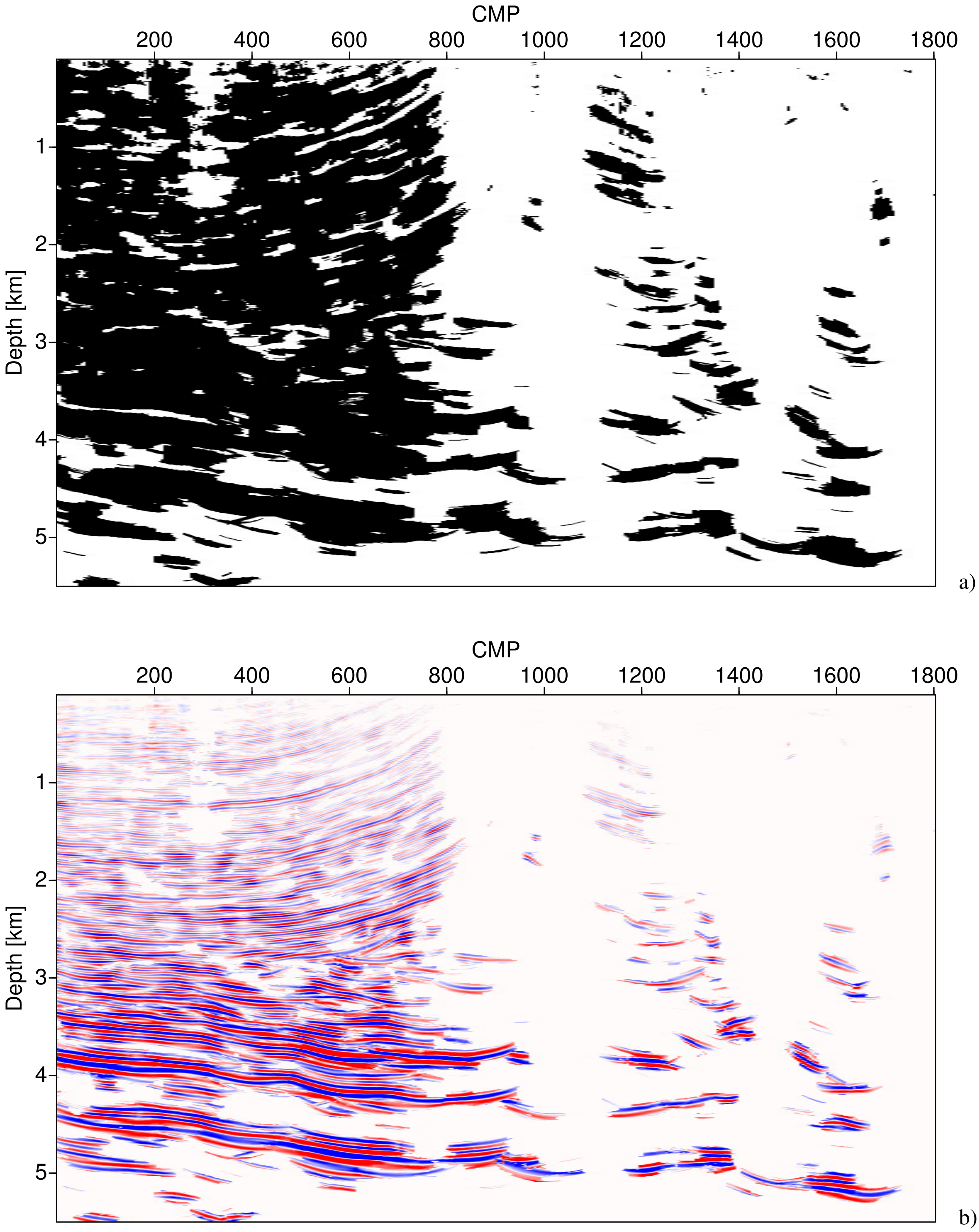

Figure 11: Locations in the migration target zone for which a stationary point has been found (black) a). Only for these locations the limited-aperture depth migration is performed b).

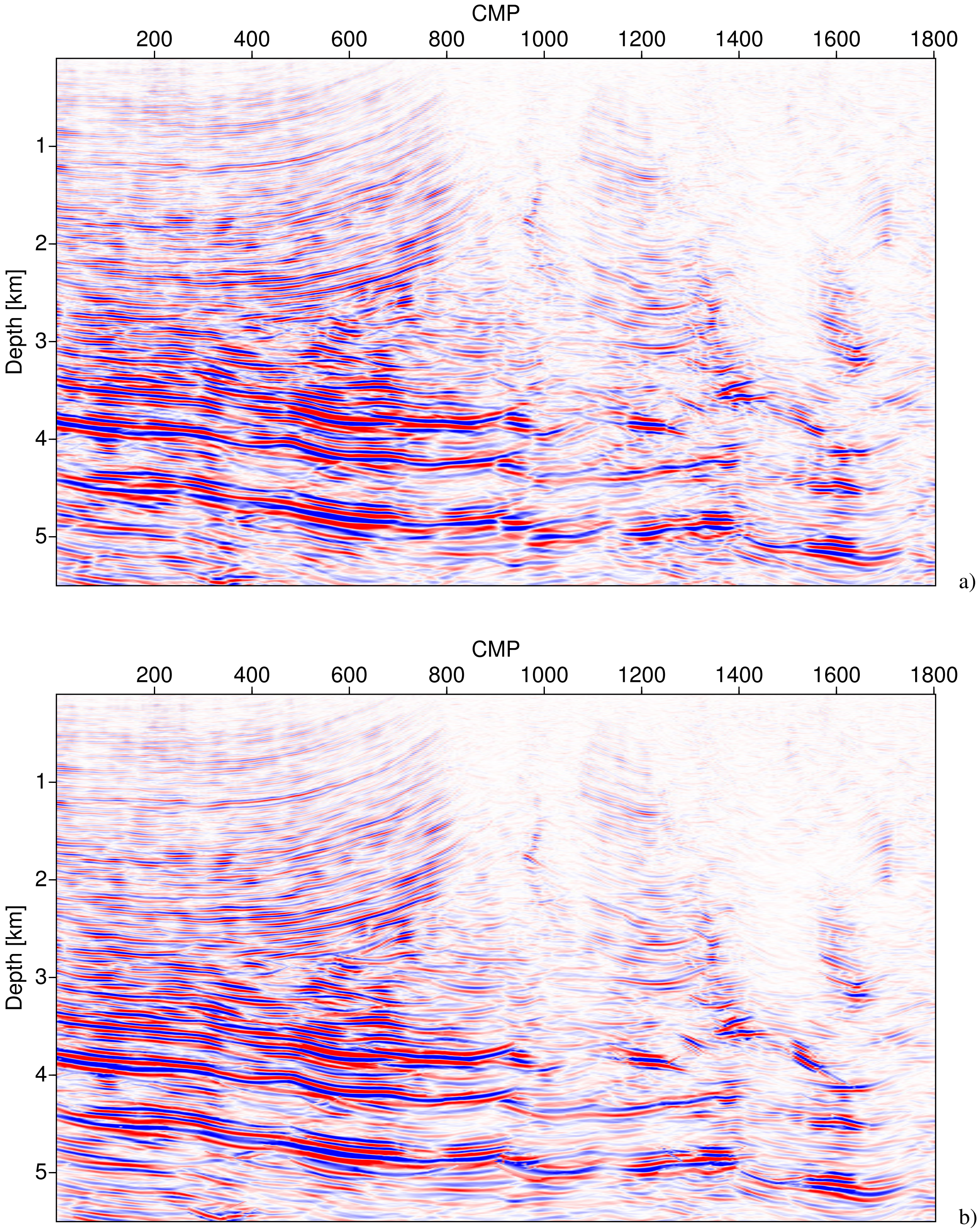

Figure 12: Result of the Kirchhoff poststack depth migration with a) conventional user-defined aperture and b) with minimum aperture. The minimum-aperture migration was performed at all locations where a stationary point has been found. At all other locations the user-given aperture is used.

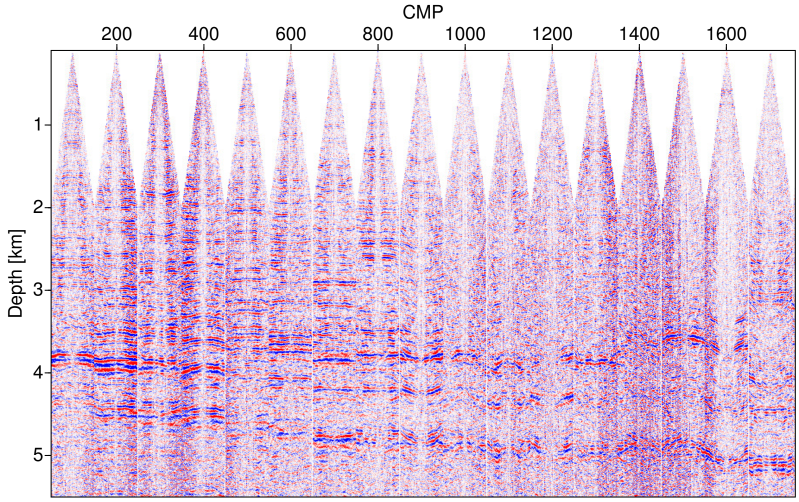

Figure 13: Several common-image gathers extracted from the conventional depth migration prestack data. The maximum offset is 3 km. Many events are horizontal while others show a moveout. Thus, the velocity model used for depth migration can still be improved.

However, due to the fact that poststack migration is by far faster than prestack migration, the run time difference between limited-aperture and conventional migration is of little practical relevance, at least in the 2D case considered here.

- Depth migration:
  - Prestack depth migration: the migration with minimum aperture was four times faster than the conventional migration. This can be explained by the reduction of the number of required summations and, more important, because the search for the stationary points could be omitted as they were already calculated in the previous limited-aperture poststack depth migration. The same principle, i. e., the application of the poststack search in the prestack limited-aperture migration, could be applied to the time migration approach. However, as poststack time migration is of minor practical use, one can not assume that a poststack migration is performed prior to the prestack application in any case.
  - Poststack depth migration: the computation time was similar for both approaches. Obviously, the effect of the smaller apertures was just compensated by the computational overhead required for the search for the stationary points.

CONCLUSION

The differences between time and depth, post- and prestack migration are resumed in the following list:

- Kinematic aspects:
  - The comparison of the pre- and poststack migration results showed that the poststack migration could benefit from the higher signal-to-noise ratio of the simulated ZO-section.
  - Time migration: differences in the image of the limited-aperture and the conventional result were detected on the target reflector events. The limited-aperture results showed on the one hand a few areas with strong variations of the attributes causing fluctuations in the imaging result, but an the other hand clear improvements of the continuity of the target reflector events. However, for data sets with a higher signal-to-noise ratio the fluctuations of the attributes could be suppressed by an previous event-consistent smoothing. Generally, in areas where the attributes are stable the limited-aperture approach performed very well, whereas in the remaining parts no improvements could be achieved due to the unreliable attributes.

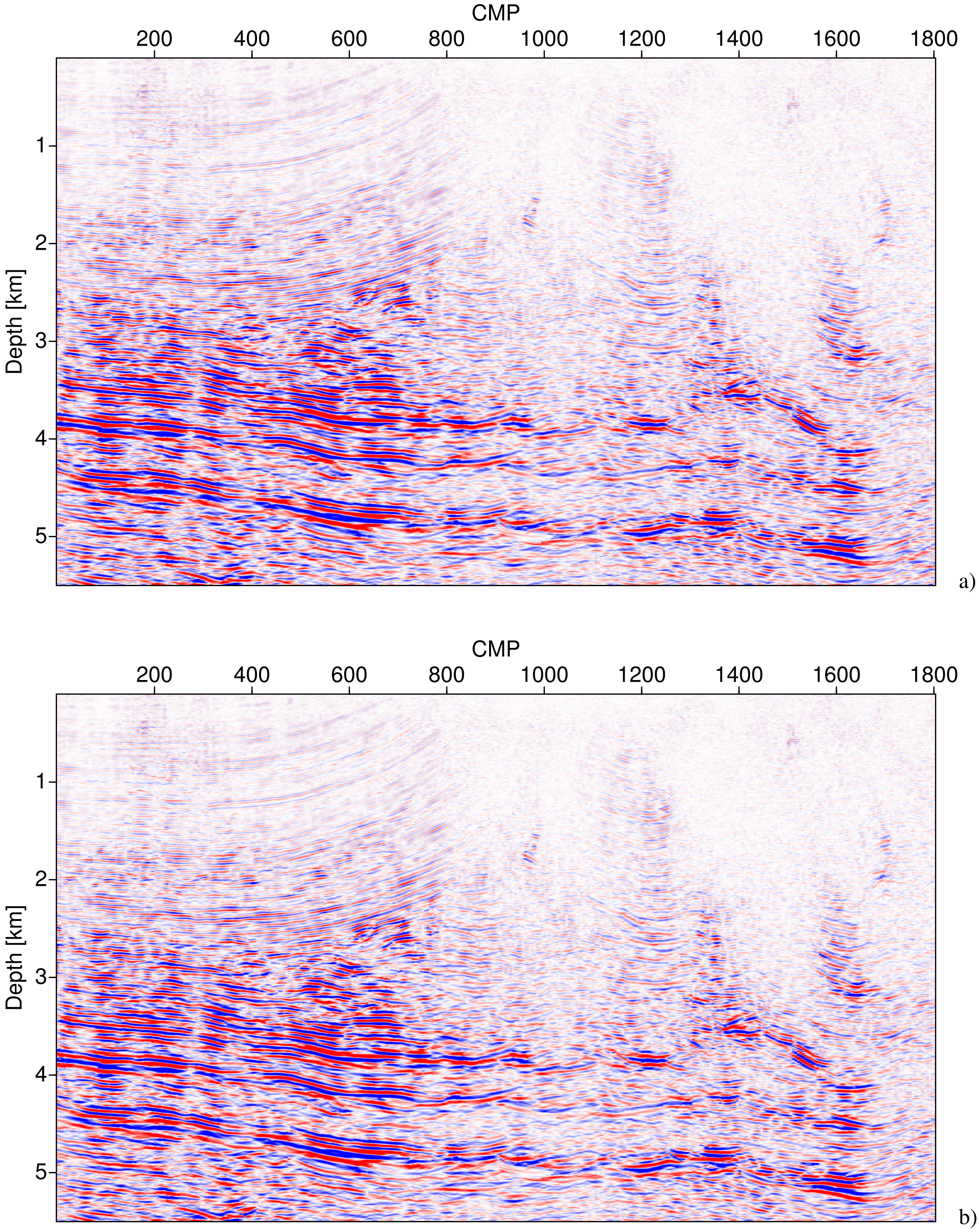

Figure 14: Result of the Kirchhoff prestack depth migration with a) conventional user-defined aperture and b) with minimum aperture. The minimum-aperture migration was performed at all locations where a stationary point has been found. At all other locations the user-given aperture is used.

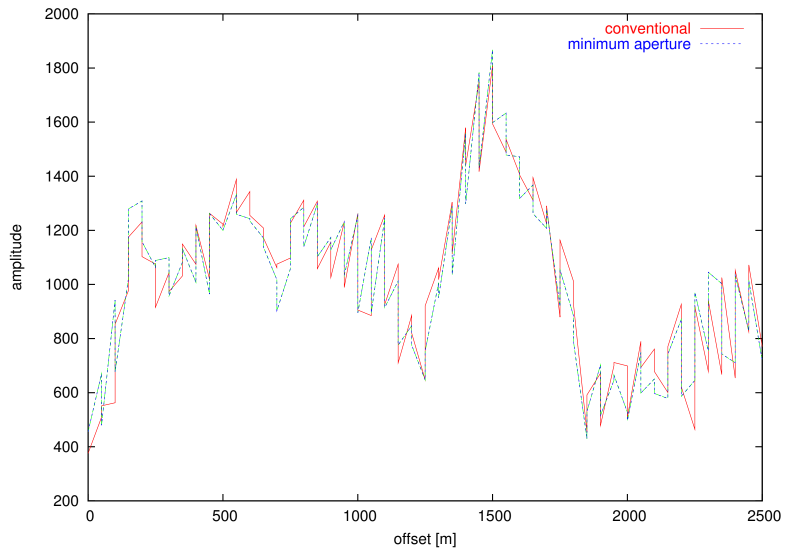

Figure 15: AVO of the strong reflector at 3.8 km extracted in the common-image gather for CMP no. 560 after true-amplitude prestack migration with minimum aperture (dashed line) and conventional aperture (solid line). Due to noise in the input data set the amplitudes fluctuate.

  - Depth migration: the effects seen in the time migration images can also be observed in the depth migration results. The increased sensitivity to errors in the depth migration velocity model explains the less distinctive improvements in the prestack migration result.

- Dynamic aspects:
  - Time migration: applications of the amplitudes like AVO analysis benefit from the reduced noise level in the limited-aperture migration result.
  - Depth migration: the effect of the incorrect depth migration model on the amplitudes obscured the effect of the different apertures considered for migration. Therefore, there is no obvious improvement in the AVO plot.

The main advantages of the limited-aperture migration can be seen in time migration, where the impact of the quality of the velocity model upon the migration result is minor. Especially in areas where AVO analyses are carried out, limited-aperture migration is a strong alternative to conventional migration. In addition, the shorter computational time is an advantage of the limited-aperture migration.

ACKNOWLEDGEMENTS

This work was kindly supported by the sponsors of the *Wave Inversion Technology (WIT) Consortium*, Karlsruhe, Germany.

REFERENCES

Duveneck, E. (2004). Velocity model estimation with data-derived wavefront attributes. *Geophysics*, 69(1):265–274.

Jäger, C. (2005). Minimum-aperture Kirchhoff migration by means of CRS attributes. In *Extended abstracts, 67th Conf.* Eur. Assn. Geosci. Eng. Session F042.

Spinner, M. and Mann, J. (2006). True-amplitude CRS-based Kirchhoff time migration for AVO/AVA analysis. *J. Seis. Expl.*, 15(2):133–152.